International Journal of Research in Engineering and Science (IJRES)
ISSN (Online): 2320-9364, ISSN (Print): 2320-9356
www.ijres.org Volume 14 Issue 4 ǁ April 2026 ǁ PP. 01-07

Proteomic Analysis of Proteins Derived from Plasma Exosomes in Alzheimer's Disease

Yanglan Hu[1], Nan Hu[1*], Xiaolian Chen[1], Shuai He[1]
[1] *College of Chemical Engineering, Sichuan University of Science & Engineering, Zigong 643002, China*
**Corresponding Author: Nan Hu*

Abstract
This study aims to identify novel biomarkers associated with Alzheimer's disease (AD) through plasma exosome proteomics analysis. As key mediators of intercellular communication, exosomes can transport specific protein complexes originating from the central nervous system across the blood-brain barrier and persist stably in plasma, thereby accurately reflecting the pathophysiological state of neurons. In this study, exosomes were first isolated and purified from plasma samples of AD patients and healthy controls using ultracentrifugation, and their morphology and marker proteins were characterized via transmission electron microscopy (TEM) and Western blot analysis. Subsequently, high-resolution liquid chromatography–tandem mass spectrometry (LC-MS/MS) was employed to perform comprehensive identification and quantitative analysis of the extracted exosomal proteins. Using bioinformatics methods, we screened for differentially expressed proteins and performed GO functional enrichment and KEGG pathway analyses to construct an AD-associated exosomal protein interaction network. The results of this study are expected to reveal potential molecular pathological features in the peripheral blood of AD patients, providing new clues and a theoretical basis for the early diagnosis and pathogenesis research of AD.

KEYWORDS: *Exosomes, Alzheimer's disease, Proteomic Analysis of Proteins*

Date of Submission: 20-03-2026 Date of Acceptance: 03-04-2026

I. Research Background

Alzheimer's disease (AD) is a common neurodegenerative disorder of the central nervous system, accounting for approximately 60–70% of dementia cases, with a disease course lasting more than ten years[1, 2]. Clinically, it manifests as progressive cognitive impairment: early-stage impairment of recent memory, mid-stage behavioral and psychological changes, and late-stage complete dementia[3]. With an aging population, it has become a leading cause of disability and death among the elderly worldwide. The pathogenesis of AD remains incompletely understood, but typical pathological changes include intracerebral β-amyloid plaques and tau protein neurofibrillary tangles, which ultimately lead to neuronal death[4]. The disease results from the combined effects of genetics, lifestyle, and environmental factors, and currently has no cure. Diagnosis poses significant challenges: early symptoms are difficult to distinguish from normal aging, making misdiagnosis highly likely; diagnostic uncertainty persists[5]. Although biomarker methods, such as cerebrospinal fluid testing and PET imaging, are effective, their invasiveness or high cost hinders widespread adoption. Currently, clinical practice relies on symptom assessment, scales, and imaging studies; however, these methods are insensitive to early, subtle lesions, resulting in most patients being diagnosed only in the moderate to late stages, thereby missing the optimal window for intervention[6]. Therefore, there is an urgent need to identify sensitive, effective, and non-invasive biomarkers to enable the early diagnosis and screening of AD[7-13].

Exosomes are a type of extracellular vesicle (EV) secreted by all cells in the brain—including neurons, microglia, and astrocytes—and play a crucial role in cell-to-cell communication[14-17]. In the central nervous system (CNS), exosomes not only transmit signals over short distances within cells but also circulate throughout the brain via cerebrospinal fluid (CSF). Consequently, exosomes and their components play a role in nervous system physiology and neurodegenerative diseases, such as Alzheimer's disease (AD, Parkinson's disease (PD), and Huntington's disease (HD)[18].

Exosomal proteins offer significant advantages as biomarkers for AD, addressing the limitations of traditional diagnostic methods. Exosomes are highly stable with a long half-life and can carry key pathological markers of AD, such as β-amyloid (Aβ1-40/Aβ1-42) and phosphorylated tau protein (p-tau181, p-tau396, etc.), reflecting pathological changes within the brain[19-21]. Using ultra-sensitive technologies such as the immunomagnetic exosome PCR platform, precise detection of early-stage AD can be achieved[22]. Furthermore, blood sample collection is non-invasive, making it suitable for large-scale screening[23].

In recent years, exosomes, as important carriers of intercellular signaling, have played a key role in the

pathogenesis of various diseases[24]. Particularly in AD, studies have found that differential proteins in serum exosomes are closely associated with the onset and progression of the disease[25]. Studies utilizing serum exosome proteomics have identified differential proteins capable of distinguishing AD patients from healthy controls with high accuracy[26]. Linear correlation analysis indicates their potential as biomarkers. Therefore, screening for differentially expressed molecules in patient tissues through omics research represents a strategy with significant potential for the early diagnosis and treatment of AD[24].

Currently, research on non-invasive biomarkers for the early diagnosis of AD remains relatively limited[19]. Therefore, this study aims to analyze the proteomics of serum exosomes from AD patients and healthy controls to identify differentially expressed proteins and investigate their roles in AD pathology, thereby providing a new approach for early AD screening.

II. Materials and Methods

2.1. Serum Sample Collection and Exosome Isolation

Serum samples were collected from patients with Alzheimer's disease and age-matched healthy volunteers at the Fifth People's Hospital of Zigong. The study was approved by the ethics committee, and all participants or their legal guardians provided written informed consent. Fasting whole blood (4 mL) was collected into EDTA-containing tubes, centrifuged at 1500×g for 10 minutes at 4°C within 2 hours, and the serum was aliquoted and stored at −80°C.

Exosomes were isolated by differential ultracentrifugation. Thawed serum was centrifuged twice at 1500×g (4°C) to remove debris, then ultracentrifuged at 100,000×g for 70 minutes at 4°C to obtain a crude pellet. The pellet was resuspended in PBS and subjected to a second ultracentrifugation under the same conditions. Purified exosomes were resuspended in PBS, aliquoted, and stored at −80°C.

Exosome morphology was examined by transmission electron microscopy, and expression of the marker protein CD63 was confirmed by Western blot to verify integrity and purity.

2.2 Western Blot

To verify exosome purity and marker expression, Western blot was performed. Exosome pellets were lysed in RIPA buffer (Beyotime), and total protein was quantified using a BCA kit. Equal amounts (20–30 μg) were separated by 10% SDS-PAGE and transferred onto 0.22 μm PVDF membranes. Membranes were blocked with 5% skim milk in TBST for 1 hour at room temperature, then incubated overnight at 4°C with rabbit anti-human CD63 (1:1000) as an exosome marker and rabbit anti-human Calnexin (1:1000) as an endoplasmic reticulum negative control. After washing, membranes were incubated with HRP-conjugated secondary antibody for 1 hour, and protein bands were visualized using ECL chemiluminescence..

2.3 Transmission Electron Microscopy (TEM)

To observe the morphological characteristics and size distribution of the extracted exosomes, negative staining was performed using transmission electron microscopy (TEM). Carefully dispense 10 μL of the exosome suspension onto a copper grid covered with a Formvar film and allow it to stand at room temperature for 10 minutes to ensure the exosomes fully adhere to the grid surface. After adsorption, gently rinse the copper grid with sterile deionized water to remove unbound sample and salt crystals. Subsequently, the sample was negatively stained using a 2% (w/v) uranyl acetate solution for 1 minute to enhance image contrast. After staining, the copper grid was allowed to air-dry at room temperature. The prepared sample was then examined under a transmission electron microscope (Hitachi, Tokyo, Japan).

2.4 Proteolysis and Peptide Desalting

Take an appropriate amount of protein sample, add dithiothreitol (DTT) to a final concentration of 5 mM, mix well, and incubate at 37°C for 1 hour for reduction. Then allow the sample to return to room temperature. Add iodoacetamide (IAA) to a final concentration of 10 mM, and incubate at room temperature in the dark for 45 minutes for alkylation modification. Dilute the sample 4-fold with 25 mM ammonium bicarbonate solution to reduce the urea concentration. Add sequencing-grade trypsin at a trypsin-to-protein mass ratio of 1:50 and incubate overnight (12–16 h) at 37°C for proteolysis. After proteolysis, add formic acid to adjust the pH to below 3 to terminate the reaction. Desalt the peptide mixture using a C18 desalting column: first activate the column with 100% acetonitrile, then equilibrate it with 0.1% formic acid; load the acidified peptide sample onto the column and wash with 0.1% formic acid to remove impurities; Finally, elute the peptides with 70% acetonitrile, collect the eluate, freeze-dry it, and store for later use.

2.5 Liquid Chromatography-Tandem Mass Spectrometry (LC-MS/MS) Analysis

Prepare mobile phases A (water + 0.1% formic acid) and B (80% acetonitrile + 0.1% formic acid). Take the lyophilized peptide sample, add 10 μL of mobile phase A to dissolve completely, centrifuge at 14,000×g for 20 min at 4°C, and collect the supernatant for later use. Accurately pipette a volume of supernatant equivalent to

1 μg of peptide and inject it for LC-MS/MS analysis. The LC elution gradient conditions are shown in Table 1.

Mass spectrometry analysis was performed using a Q Exactive HF-X mass spectrometer (Thermo Fisher Scientific) equipped with a Nanospray Flex™ (NSI) ion source. The ion source parameters were set as follows: spray voltage 2.2 kV, ion transfer tube temperature 320°C. Data acquisition was performed in data-dependent acquisition (DDA) mode: full scan range m/z 350–1500, first-stage mass resolution set to 120,000 (at m/z 200), automatic gain control (AGC) target set to 3×10^6, and maximum injection time set to 80 ms. The top 40 parent ions with the highest ion intensity in the full scan were selected for secondary fragmentation via high-energy collision dissociation (HCD), with the collision energy (NCE) set to 27%. Set the MS/MS resolution to 15,000 (at m/z 200), the AGC target value to 5×10^4, and the maximum injection time to 45 ms. Raw mass spectrometry data is collected and saved in real time by the instrument control system.

Table 2-1 Separation Gradient

Time（min）	Proportion of mobile phase B（%）
0	5
5	12
39	30
49	40
50	95
60	95

Table 2-2 Search Parameters

Parameters	Value
Enzyme	Trypsin
Static Modification	Carbamidomethyl(C)
Dynamic Modification	MOxidation(15.995Da); Acetyl (Protein N-termin)
Precursor ion mass tolerance	± 15 ppm
Fragment ion mass tolerance	± 0.02Da
Max Missed Cleavages	2

2.6. Identification and Screening of Differentially Expressed Proteins

Differential analysis was performed using the t-test, with a cutoff of p-value ≤ 0.05 and a fold change ≥ 1.2-fold, yielding the results for differentially expressed proteins.

2.6. Bioinformatics Analysis

To further understand the biological functions of the differentially expressed proteins, the identified proteins were imported into the Gene Ontology (GO) and Kyoto Encyclopedia of Genes and Genomes (KEGG) databases to annotate their potential biological functions.

III. Results

3.1 Identification of Plasma Exosomes

Exosomes were isolated from serum using ultracentrifugation and further characterized for their morphology and marker proteins via TEM and Western blot analysis. TEM results showed that the isolated vesicles exhibited the typical cup-shaped or spherical membrane structure characteristic of exosomes. Western blot analysis further confirmed that these vesicles expressed the exosome marker protein CD63, while the endoplasmic reticulum marker calnexin was negative. Taken together, these results indicate that this study successfully isolated high-purity exosomes from serum using ultracentrifugation.

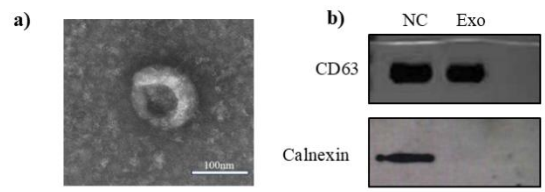

Figure 1: Identification of plasma-derived exosomes

a) Electron micrograph of exosomes following negative staining; b) Western blot analysis of characteristic exosomal membrane proteins

3.2 Sequencing of Plasma Exosomal Proteins

To demonstrate differences in the expression levels of plasma exosomal proteins between Alzheimer's disease patients and healthy controls, we performed protein quantification on the extracted exosomes using a label-free method. Statistical analysis of the raw sequencing results revealed that the number of proteins detected per sample was similar across all samples. Venn diagram analysis of the proteins identified in each group showed significant differences between groups. Venn diagram analysis of the proteins identified in each sample within a group indicated that intragroup variability was minimal. Principal Component Analysis (PCA) revealed that, in the three-dimensional PCA plot, samples from the control group (Group D) were far from those of the experimental group (Group S), indicating significant differences between the two groups. Meanwhile, the close proximity of samples within the same group suggests good reproducibility. This indicates that the sample processing steps were well-defined and the data quality is reliable, providing a solid foundation for subsequent screening of differentially expressed proteins.

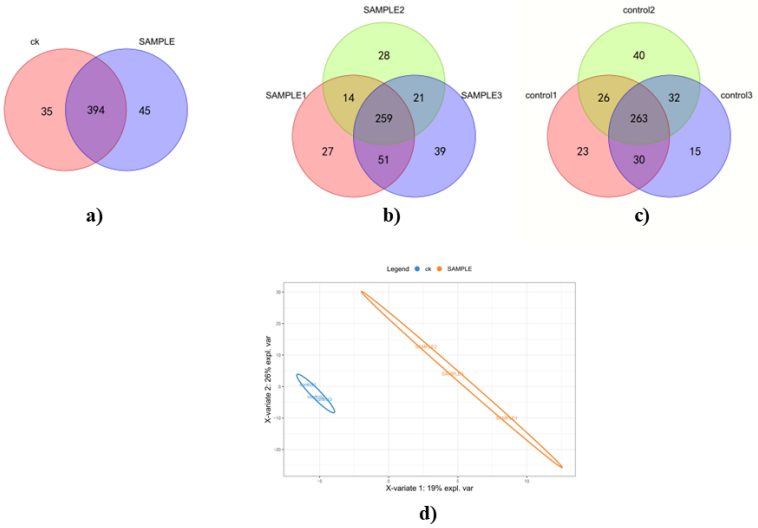

Figure 2 Protein Analysis Results

a) Venn diagram comparing sample groups; b) Venn diagram within the AD sample group; c) Venn diagram within the NC sample group; d) PLS-DA plot

3.3. Analysis of Differentially Expressed Proteins in Plasma Exosomes

Following sequencing analysis and data normalization of plasma exosome proteins, we identified a total of 620 known proteins in plasma exosome samples from Alzheimer's disease patients and healthy controls. Using a screening threshold of $|\log_2$ fold change > 1.2 and $p < 0.05$, we identified 5 differentially expressed proteins, including 1 downregulated protein and 4 upregulated proteins. The results are shown in the figure, where the x-axis represents log2(fold change) and the y-axis represents -log10(p-value). Each data point represents a protein, and the color indicates whether the protein is differentially expressed. The two dashed lines on the x-axis represent cut-off values for FC; the left and right lines correspond to FC < 1/1.2 and FC > 1.2, respectively. The dashed line on the y-axis represents the p-value cut-off; data points above this line indicate p-values < 0.05. Combining the FC and p-value metrics, red points in the upper-right quadrant represent upregulated differentially expressed proteins, while green points in the upper-left quadrant represent downregulated differentially expressed proteins.

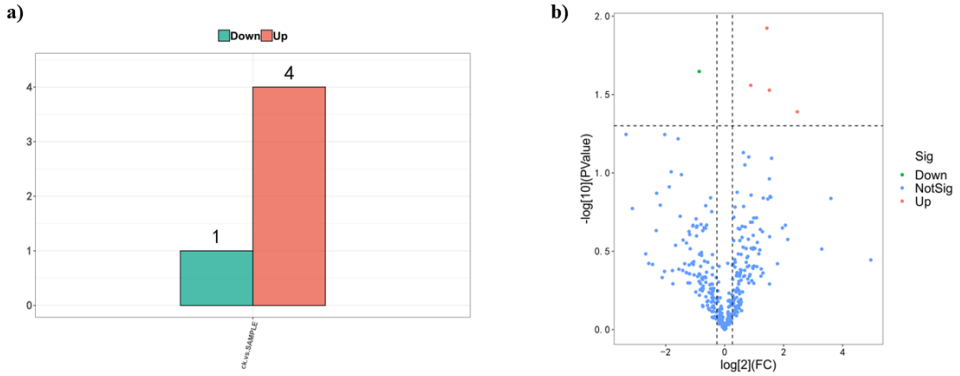

Figure 3: Differential protein analysis chart

a) Bar chart of differentially expressed proteins; b) Volcano plot of differentially expressed proteins

3.4. Functional Enrichment Analysis

To further investigate the biological functions of differentially expressed proteins, Gene Ontology (GO) functional annotation analysis was performed on the top 20 most enriched proteins, covering three dimensions: biological processes (BP), cellular components (CC), and molecular functions (MF). The results showed that the enriched pathways are highly associated with the core pathological mechanisms of Alzheimer's disease (AD).

At the biological process level, the most significantly enriched terms included activation of the classical complement pathway, immunoglobulin-mediated immune responses, and innate immune responses. This finding directly corroborates the central role of neuroinflammation in AD pathology. Furthermore, the enrichment of hydrogen peroxide degradation suggests impaired reactive oxygen species (ROS) clearance in AD, which may be associated with reduced catalase activity, leading to oxidative damage to neuronal lipids and proteins and accelerating Aβ deposition and tau protein hyperphosphorylation.

Molecular functional enrichment analysis reveals the proteinopathological characteristics of AD. The enrichment of protein self-assembly functions directly corresponds to the β-folding aggregation tendency of Aβ (oligomer and plaque formation) and the abnormal aggregation of tau protein (neurofibrillary tangles). The enrichment of microtubule-binding function suggests Tau protein dysfunction: in AD, excessive Tau phosphorylation leads to the loss of its microtubule-binding ability, triggering microtubule disassembly and axonal transport impairment, ultimately resulting in neuronal apoptosis. Furthermore, the enrichment of serine protease inhibitor activity suggests that reduced activity of such inhibitors (e.g., α1-antitrypsin) may weaken the suppression of synaptic protein degradation, thereby disrupting synaptic structural integrity and exacerbating cognitive impairment.

In summary, the results of the GO enrichment analysis systematically reveal the functional enrichment patterns of AD-associated proteins in exosomes. These findings reflect the core pathological mechanisms of AD from multiple dimensions, including neuroinflammation, oxidative stress, synaptic dysfunction, and protein pathology, providing key insights for a deeper understanding of the disease's progression.

We further conducted KEGG enrichment analysis on the genes. In the figure, the x-axis represents the odds ratio, the y-axis represents each KEGG pathway term, color indicates enrichment level (-log10(P-value)), and circle size indicates the number of genes: Red dots in the figure represent pathways with high significance (small p-values) or high gene coverage, which may be directly associated with the core pathology of AD. Phagosomes regulate the key pathway by which microglia phagocytose Aβ; carbon metabolism reflects abnormalities in brain energy metabolism in AD, leading to insufficient neuronal ATP and increased apoptosis; the HIF-1 pathway is associated with cerebral hypoxia and amplified inflammation, while platelet activation involves vascular risks. Taken together, these pathways—which involve impaired Aβ clearance, synaptic loss, and metabolic inflammation—are expected to become key areas of focus for research into the mechanisms of AD and for therapeutic interventions.

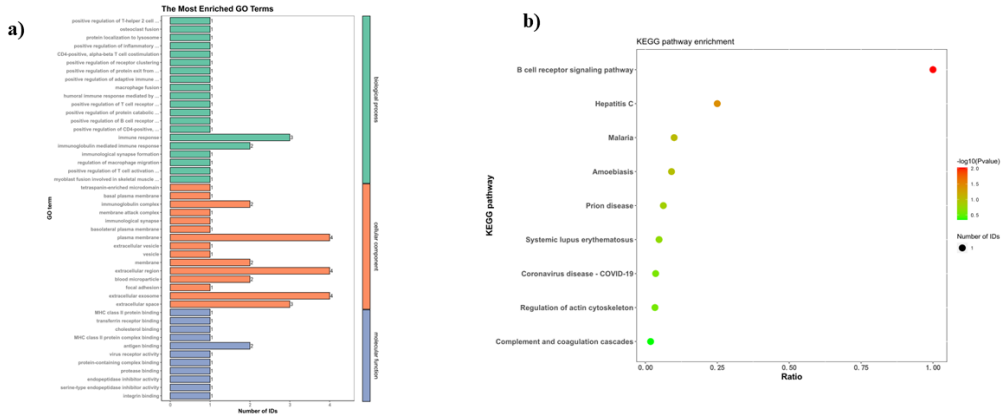

Figure 4 Analysis of Differential Expression Between Groups

a) GO functional enrichment analysis of differentially expressed proteins between groups; b) KEGG pathway analysis of differentially expressed proteins between groups

IV. Discussion

In this study, label-free proteomics was used to analyze serum exosomes from Alzheimer's disease (AD) patients and healthy controls. Five differentially expressed proteins (four upregulated, one downregulated) were identified.

Quality control confirmed reliable results: TEM showed typical cup-shaped exosome morphology; Western blot confirmed CD63 positivity and calnexin negativity, indicating high purity; PCA showed clear separation between AD and control groups with good intra-group clustering.GO functional enrichment linked differentially expressed proteins to core AD pathologies. Biological processes included activation of the classical complement pathway and immunoglobulin-mediated immune responses, supporting the role of neuroinflammation in AD. Enrichment of the hydrogen peroxide degradation pathway indicated oxidative stress imbalance, which can promote Aβ aggregation and Tau pathology.Cellular component analysis revealed enrichment in glutamatergic synapses (implicated in early cognitive decline), endosomal vesicles (involved in Aβ production/clearance), and tight junctions—suggesting possible blood-brain barrier compromise and peripheral-central immune crosstalk in AD.PCA analysis showed clear separation between the AD group and the control group, while samples within each group clustered well, confirming the consistency of sample processing and the reliability of data quality, thereby providing a solid foundation for subsequent differential protein screening[7, 8].

KEGG pathway enrichment highlighted additional mechanisms: phagosome pathway (possible microglial dysfunction in Aβ clearance), focal adhesion (affecting microglial migration and synaptic stability), carbon metabolism (supporting the "type 3 diabetes" hypothesis), HIF-1 pathway (hypoxia-inflammation loop), and platelet activation (vascular contributions).

Overall, serum exosome proteomics revealed AD-associated proteins and pathways spanning neuroinflammation, oxidative stress, synaptic dysfunction, metabolic abnormalities, and vascular factors. These findings provide potential candidate biomarkers for early diagnosis and a theoretical basis for targeted interventions. The differential expression of tight junction-associated proteins suggests that the integrity of the blood-brain barrier may be compromised in AD, leading to the infiltration of peripheral immune cells and Aβ into the central nervous system and amplifying neuroinflammatory responses[7-10]. This finding provides new evidence supporting the "peripheral-central interaction" hypothesis of AD.

Overall, serum exosome proteomics revealed AD-associated proteins and pathways spanning neuroinflammation, oxidative stress, synaptic dysfunction, metabolic abnormalities, and vascular factors. These findings provide potential candidate biomarkers for early diagnosis and a theoretical basis for targeted interventions.

V. Acknowledgments

This work was supported by the Sichuan Science and Technology Program （2023NSFSC1149）, Science Foundation of Sichuan University of Science & Engineering (2021RC04) ， Key Science and Technology Program of Zigong City (2025YLWS02), and Foundation of Zigong Academy of Big Data and Artificial Intelligence in Medical Science (2024-YGY-01-01).

Compliance with ethical standards

Conflict of interest

Authors declare that they have no potential conflicts of interest.

References

[1]. Cai Z-Y, Ke Z-Y, Xiao M, et al. Exosomes: a novel therapeutic target for Alzheimer's disease? [J]. Neural Regeneration Research, 2018.

[2]. Ou-Yang P, Cai Z-Y, Zhang Z-H. Molecular Regulation Mechanism of Microglial Autophagy in the Pathology of Alzheimer's Disease [J]. Aging and Disease, 2023.

[3]. Hamlett E D, Ledreux A, Potter H, et al. Exosomal biomarkers in Down syndrome and Alzheimer's disease [J]. Free Radical Biology and Medicine, 2017.

[4]. Kandimalla R, Saeed M, Tyagi N, et al. Exosome-based approaches in the management of Alzheimer's disease [J]. Neuroscience & Biobehavioral Reviews, 2022.

[5]. Jagust W, Jack C R, Bennett D A, et al. "Alzheimer's disease" is neither "Alzheimer's clinical syndrome" nor "dementia" [J]. Alzheimer's & Dementia, 2019.

[6]. Rawat P, Sehar U, Bisht J, et al. Alzheimer's disease and Alzheimer's disease-related dementias in Hispanics: Identifying influential factors and supporting caregivers [J]. Ageing Research Reviews, 2023.

[7]. Cheng L, Doecke J D, Sharples R A, et al. Prognostic serum miRNA biomarkers associated with Alzheimer's disease shows concordance with neuropsychological and neuroimaging assessment [J]. Mol Psychiatry, 2015, 20(10): 1188-1196.

[8]. Chunhui G, Yanqiu Y, Jibing C, et al. Exosomes and non-coding RNAs: bridging the gap in Alzheimer's pathogenesis and therapeutics [J]. Metabolic Brain Disease, 2025.

[9]. Iulita M F, Bejanin A, Vilaplana E, et al. Association of biological sex with clinical outcomes and biomarkers of Alzheimer's disease in adults with Down syndrome [J]. Brain Commun, 2023, 5(2): fcad074.

[10]. Krylova S V, Feng D. The Machinery of Exosomes: Biogenesis, Release, and Uptake [J]. Int J Mol Sci, 2023, 24(2).

[11]. Mathieu M, Martin-Jaular L, Lavieu G, et al. Specificities of secretion and uptake of exosomes and other extracellular vesicles for cell-to-cell communication [J]. Nat Cell Biol, 2019, 21(1): 9-17.

[12]. Wang S, Talukder A, Cha M, et al. Computational annotation of miRNA transcription start sites [J]. Brief Bioinform, 2021, 22(1): 380-392.

[13]. Xiao T, Zhang W, Jiao B, et al. The role of exosomes in the pathogenesis of Alzheimer' disease [J]. Translational Neurodegeneration, 2017.

[14]. Goetzl E J. Advancing medicine for Alzheimer's disease: A plasma neural exosome platform [J]. Faseb j, 2020, 34(10): 13079-13084.

[15]. Graff-Radford J, Yong K X X, Apostolova L G, et al. New insights into atypical Alzheimer's disease in the era of biomarkers [J]. Lancet Neurol, 2021, 20(3): 222-234.

[16]. Gurunathan S, Kang M H, Kim J H. A Comprehensive Review on Factors Influences Biogenesis, Functions, Therapeutic and Clinical Implications of Exosomes [J]. Int J Nanomedicine, 2021, 16: 1281-1312.

[17]. Wu J, Feng Z, Wang R, et al. Integration of bioinformatics analysis and experimental validation identifies plasma exosomal miR-103b/877-5p/29c-5p as diagnostic biomarkers for early lung adenocarcinoma [J]. Cancer Medicine, 2022.

[18]. Scheltens P, De Strooper B, Kivipelto M, et al. Alzheimer's disease [J]. Lancet, 2021, 397(10284): 1577-1590.

[19]. Vieira E, Nolan J, Maslanik T, et al. Liquid Brain Biopsy in Late-Life Depression and Alzheimer's Disease Using Circulating Brain-Derived Exosomes [J]. Biological Psychiatry, 2022.

[20]. Wang C, Huang W, Lu J, et al. TRPV1-Mediated Microglial Autophagy Attenuates Alzheimer's Disease-Associated Pathology and Cognitive Decline [J]. Frontiers in Pharmacology, 2022.

[21]. Wang Q, Huang X, Su Y, et al. Activation of Wnt/β-catenin pathway mitigates blood-brain barrier dysfunction in Alzheimer's disease [J]. Brain, 2022, 145(12): 4474-4488.

[22]. Liu C G, Zhao Y, Lu Y, et al. ABCA1-Labeled Exosomes in Serum Contain Higher MicroRNA-193b Levels in Alzheimer's Disease [J]. Biomed Res Int, 2021, 2021: 5450397.

[23]. Rubenstein E, Tewolde S, Michals A, et al. Alzheimer Dementia Among Individuals With Down Syndrome [J]. JAMA Network Open, 2024.

[24]. Zhang J, Li S, Li L, et al. Exosome and exosomal microRNA: trafficking, sorting, and function [J]. Genomics, Proteomics & Bioinformatics, 2015.

[25]. Zhu L, Ma L, Du X, et al. M2 Microglia-Derived Exosomes Protect Against Glutamate-Induced HT22 Cell Injury via Exosomal miR-124-3p [J]. Molecular Neurobiology, 2024.

[26]. Muskan M, Abeysinghe P, Cecchin R, et al. Therapeutic potential of RNA-enriched extracellular vesicles: The next generation in RNA delivery via biogenic nanoparticles [J]. Mol Ther, 2024, 32(9): 2939-2949.